

A molecular dynamics investigation of dynamical heterogeneity in supercooled water

V. Teboul^{1,a}, S. Maabou¹, L.C. Fai², and A. Monteil¹

¹ Laboratoire des Propriétés Optiques des Matériaux et Applications, UMR CNRS 6136, Université d'Angers, 2 boulevard Lavoisier, 49045 Angers, France

² Department of Physics, Faculty of Science, University of Dschang, Dschang, Cameroon

Received 27 September 2004 / Received in final form 29 November 2004

Published online 15 March 2005 – © EDP Sciences, Società Italiana di Fisica, Springer-Verlag 2005

Abstract. We investigate the presence of dynamical heterogeneity in supercooled water with molecular dynamics simulations using the new water model proposed by Mahoney and Jorgensen [M.W. Mahoney, W.L. Jorgensen *J. Chem. Phys.* **112**, 8910 (2000)]. Prompted by recent theoretical results [J.P. Garrahan, D. Chandler, *Phys. Rev. Lett.* **89**, 35704 (2002)] we study the dynamical aggregation of the least and the most mobile molecules. We find dynamical heterogeneity in supercooled water and string-like dynamics for the most mobile molecules. We also find the dynamical aggregation of the least mobile molecules. The two kinds of dynamical aggregation appear however to be very different. Characteristic times are different and evolve differently. String-like motions appear only for the most mobile molecules, a result predicted by the facilitation theory. The aggregation of the least mobile molecules is more organized than the bulk while the opposite is observed for the most mobile molecules.

PACS. 64.70.Pf Glass transitions – 61.20.Lc Time-dependent properties; relaxation

1 Introduction

The investigation of water is important for the understanding of many technological and biophysical processes. Water is also one of the most ‘fragile’ liquids [1] in Angell’s classification [2,3] of glass-formers. However water has been reported to become ‘strong’ [1,4] at very low temperatures. The comprehension of supercooled water is then important for the understanding of fragility. ‘Fragility’ is often associated with the increase of a correlation length with temperature decrease [5–7]. The existence of dynamical heterogeneity is expected to be at the origin of this correlation length [5,8]. Dynamical heterogeneity has been observed experimentally and using molecular dynamics (MD) simulations in various glass formers and spin glasses [5,9]. From MD simulations these heterogeneities are usually characterized by an aggregation of the most mobile molecules [10–13]. Heterogeneities observed in NMR hole burning experiments correspond however to molecules of low mobility [9]. In a recent theory [14], molecules of low and high mobility are expected to be at the origin of the strange behavior of glass-formers. Molecules of low mobility are also expected to be of great importance in the ‘frustration limited domain theory’ [6]. The observation of the behavior of low mobility molecules in supercooled water and its comparison with the behavior of high mobility molecules is then of great interest to us.

The presence of an aggregation of low mobility molecules may also give information on the conditions that preside to crystallization in supercooled water.

In this article we use MD simulations with the recent TIP5P potential [15] to study supercooled water. This new potential has been found to be closer to real water than previously proposed pair-wise additive potentials [15–17]. We checked that no crystallization occurs during our simulations [18]. We find dynamical heterogeneity in supercooled water together with string-like dynamics for the most mobile molecules. More interestingly to us we also find the dynamical aggregation of the least mobile molecules. The characteristic time corresponding to this kind of heterogeneity increases very rapidly when temperature decreases. The two kind of dynamical aggregation appear to be very different. Characteristic times are different and evolve differently. String-like motions [9,19,20] appear only for the most mobile molecules. The aggregation of the least mobile molecules is more organized than the bulk while the opposite is observed for the most mobile molecules. This article is organized as follows: in Section 2 we describe the simulation procedure, in Section 3 we discuss the different results and Section 4 is the conclusion.

2 Calculation

The present simulations were carried out for a system of 507 molecules (507 O + 1014 H). We used the TIP5P

^a e-mail: victor.teboul@univ-angers.fr

potential [15,16], which reproduces well the structural and dynamical properties of water [16,17]. We used the densities calculated in reference [16] and corresponding to a constant atmospheric pressure for this potential. The equations of motions were integrated with a Gear algorithm [21] and the quaternions method [21]. The time step was chosen equal to 10^{-15} s. The reaction field method [21] was employed to take into account long-range electrostatic interactions in the same conditions than described in references [15,16]. The system is heated at a temperature of 300 K to insure homogenization; then it is cooled to the different temperatures of study with a Berendsen thermostat [22] and stabilized during 10 ns for the lowest temperatures studied. After stabilization the configurations are recorded during 10 ns and the autocorrelation functions are then calculated from these configurations. We checked that no crystallization occurred during these last 10 ns.

In the Markovian approximation the self Van Hove correlation function $G_s(r, t)$,

$$G_s(r, t) = \frac{1}{N} \cdot \sum_i \delta(r - (|\mathbf{r}_i(t) - \mathbf{r}_i(0)|)) \quad (1)$$

which represents the probability for a particle to be at time t at a distance r from its earlier position at time 0, has a Gaussian form. Departure from this Gaussian form has been found in various glass forming liquids and is thought to be due to dynamical heterogeneities. Such deviations are usually characterized by the Non-Gaussian parameter:

$$\alpha_2(t) = 3/5 \langle r^4(t) \rangle / \langle r^2(t) \rangle^2 - 1 \quad (2)$$

where $\langle r^2(t) \rangle$ is the mean square displacements

$$\langle r^2(t) \rangle = \frac{1}{NN_{t_0}} \cdot \sum_{i, t_0} (|\mathbf{r}_i(t + t_0) - \mathbf{r}_i(t_0)|)^2 \quad (3)$$

and $\langle r^4(t) \rangle$ is defined by the relation:

$$\langle r^4(t) \rangle = \frac{1}{NN_{t_0}} \cdot \sum_{i, t_0} (|\mathbf{r}_i(t + t_0) - \mathbf{r}_i(t_0)|)^4. \quad (4)$$

The Non-Gaussian parameter reaches a maximum for a characteristic time usually named t^* . t^* evolves with temperature and is thought to be a characteristic of the heterogeneity. However we define in this article the times that correspond to the maximum of the aggregations as the characteristic times of the heterogeneities. We then define the mobility μ_i of the molecule i by the relation:

$$\mu_i(t) = (r_i^2(t) / \langle r^2(t) \rangle)^{0.5}. \quad (5)$$

We then select molecules of high and low mobility for the calculation of dynamical heterogeneity. This selection is then dependent on the time t chosen in the definition of the mobility $\mu_i(t)$. When not specified we use as usual the time t^* corresponding to the maximum of the Non-Gaussian parameter as the characteristic time in this procedure. However we show in this article that if the characteristic time corresponding to the most mobile molecules is equal to t^* , this is not the case for the least mobile molecules. We then define another characteristic time t^- that corresponds to the maximum of the aggregation of the least mobile molecules.

3 Results

This section is organized as follows: In a first part we investigate the presence of dynamical heterogeneity in supercooled water. We show the aggregation of the most mobile molecules (MMM) and the aggregation of the least mobile molecules (LMM). Then we compare the different characteristics of these two kinds of heterogeneity. We study the characteristic times associated with these heterogeneities, and the evolution of the aggregations with temperature. Then we investigate the presence of string-like dynamics [9,19,20] associated with the different heterogeneities and finally the angular organization of the two kinds of aggregations.

A simple method to investigate the presence of dynamical heterogeneity is to calculate the radial distribution function (RDF) for molecules of different mobility. This function $g(r)$ represents the probability to find the center of mass of a molecule at a distance r from the center of mass of another molecule. This function is also equal to the distinct Van Hove correlation function at time zero $G(r, 0) = g(r)$. If the RDF ($G(r, 0)$) corresponding to molecules of different mobility are different, then dynamical heterogeneities are present. Figure 1a shows the RDF between mean molecules of water (continuous line) together with the RDF between the 6 percent most mobile water molecules (full circles) and the 6 percent least mobile molecules (dashed line). The three RDF differ. This result shows the presence of dynamical heterogeneities in supercooled water. Moreover the peak values for the most mobile molecules are higher than the corresponding peaks for the mean molecules. This increase persists up to the fourth neighbor and can be interpreted as the signature of an aggregation of the most mobile molecules. The same increase is observed for the least mobile molecules. We deduce then the occurrence of two kinds of aggregations, an aggregation of the least mobile molecules (LMM) and also an aggregation of the most mobile molecules (MMM).

We can see in Figure 1a that the aggregation of the MMM corresponds to molecules less organized than the mean molecules: the RDF of the most mobile molecules decreases much less, between the different peaks corresponding to the most probable positions, than the RDF of the mean. In contrast, the aggregation of the least mobile molecules is more organized than the bulk at the same temperature: the RDF vanishes almost to zero between the first peaks. However the structure observed in Figure 1a for the LMM is still the structure of liquid water since the positions of the peaks do not change, the width of the peaks is still important and the RDF does not totally vanish between peaks. The aggregation of the LMM corresponds neither here to crystallization nor to Low Density water. However crystallization may be favored by these aggregations [18].

In previous simulations [23] the mobility of water molecules has been related to the local structure. Molecules of high mobility have been related to a distorted local tetrahedral structure, while molecules of low mobility have been related to an approximately tetrahedral local

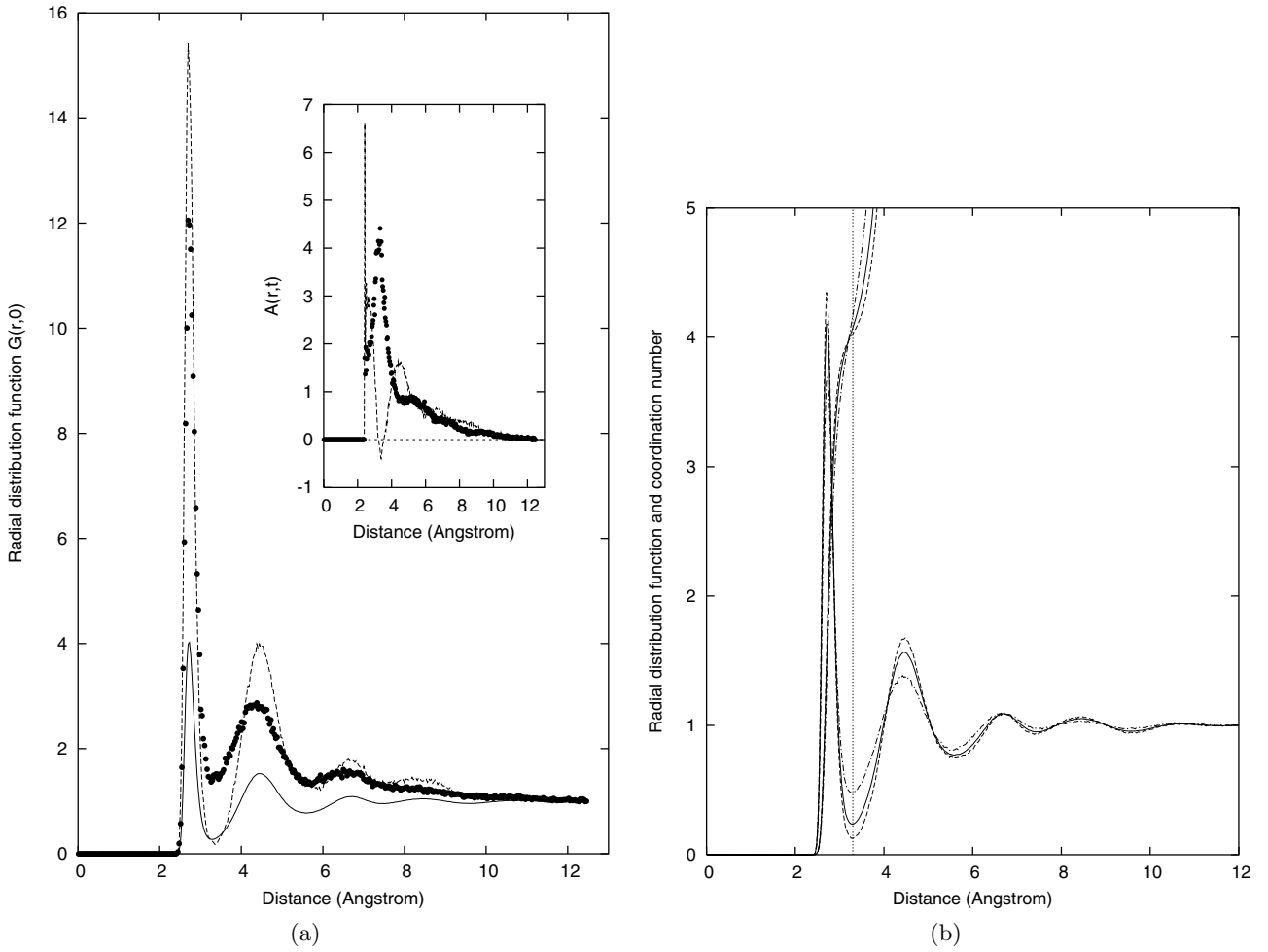


Fig. 1. (a) Radial distribution function between the centers of mass of: the 6 percent most mobile water molecules $G_{mm}(r,0)$ (full circles), the 6 percent least mobile water molecules $G_{lm}(r,0)$ (dashed line) or mean water molecules $G(r,0)$ (continuous line) at a temperature of 240 K. The 6 percent most or least mobile molecules are selected from the mobility of each molecule i : $\mu_i(t)$ with $t = t^* = 28$ ps for the most mobile molecules and $t = t^- = 500$ ps for the least mobile molecules. Inset: Functions $A^+(r, t^*) = G_{mm}(r,0)/G(r,0) - 1$ (full circles) and $A^-(r, t^-) = G_{lm}(r,0)/G(r,0) - 1$ (dashed line) at a temperature of 240 K. r represents here the distance between the centers of mass of two water molecules. The dotted line corresponds to the axis. (b) Radial distribution function between the centers of mass of: the 6 percent most (dashed line) or least (dotted line) mobile water molecules and the mean water molecules, at a temperature of 235 K. This function represents then the mean environment around the most mobile or the least mobile molecules. The radial distribution between the mean water molecules is also plotted for comparison (continuous line) at the same temperature. The corresponding coordination numbers are also plotted with the same lines than the radial distribution functions.

structure. This compartment has been then related to the local energy of these different structures [23].

These results open the question of a possible relation between the local structure and the dynamical aggregations observed in our simulations. We then plot in Figure 1b the radial distribution function of the whole set of water molecules surrounding molecules of low and high mobility together with the mean radial distribution function. We also plot in this figure the corresponding coordination numbers. A pure tetrahedral structure leads to a coordination number equal to 4 for the first neighbor distance. In this viewpoint we then expect a higher coordination number for molecules of high mobility. We can

see in Figure 1b that this is the case here. The most mobile molecules correspond to a local structure more distorted than the mean while the least mobile molecules correspond to a local structure less distorted than the mean. In opposition with what is observed in other glass-formers we then observe a clear correlation between the local arrangement and the dynamical heterogeneity in supercooled water. This correlation is however too weak in comparison with the results of reference [23] to lead to a simple structural explanation for dynamical heterogeneity in water. Dynamical heterogeneity seem to be favored in regions corresponding to specific local structures, the mobility being then enhanced by cooperative motions or dynamic facilitation [14].

In order to study the evolution of the aggregation of the least mobile molecules with temperature, we need to evaluate first the characteristic time (t^-) of this aggregation. Due to the mathematical form of the Non-Gaussian parameter, see equation (2), the most mobile molecules (MMM) contribution predominates in the evolution of the Non-Gaussian parameter (NGP) $\alpha_2(t)$. The contribution of the MMM is much more important in $\langle r^2 \rangle$ and in $\langle r^4 \rangle$ than the contribution of the LMM, because in the summation r_i^2 and r_i^4 is much more important if molecule i is a MMM. Then in contrast with what is observed for the MMM, t^- may be different from the characteristic time of the Non-Gaussian parameter t^* .

The mobility $\mu_i(t)$ of the molecule i is defined by the relation [5]. We then select molecules of high and low mobility for the calculation of dynamical heterogeneity. This selection of molecules of high and low mobility depends on the time t chosen in the definition of the mobility $\mu_i(t)$. We define here the function:

$$A^+(r, t) = G_{mm}(r, 0)/G(r, 0) - 1. \quad (6)$$

In this formula $G_{mm}(r, 0)$ is the radial distribution function between the centers of mass of the most mobile water molecules, and $G(r, 0)$ is the mean radial distribution function between two molecules. $A(r, t)$ gives a measure of the correlation increase between mobile molecules. Similarly we define $A^-(r, t)$ for the least mobile molecules. We can see in the inset of Figure 1a these functions $A^+(r, t^*)$ (full circles) and $A^-(r, t^-)$ (dashed line) corresponding to the most and the least mobile water molecules at a temperature of 240 K. The sizes of the aggregations (10 Angstrom in both cases) may be easily read from this figure. The negative value of $A^-(r, t^-)$ at the first minimum of the radial distribution function shows even more clearly than in Figure 1a that for short distances the aggregation of the least mobile molecules is more organized than the bulk. In contrast, the maximum value of $A^+(r, t^*)$ at the same position shows that the aggregation of the most mobile molecules is less organized than the bulk.

We then define the integrals $I^{+/-}(t)$ of the functions $A^{+/-}(r, t)$ by:

$$I^+(t) = N/V \int_0^\infty A^+(r, t) 4\pi r^2 dr \quad (7)$$

$$I^-(t) = N/V \int_0^\infty |A^-(r, t)| 4\pi r^2 dr. \quad (8)$$

In our notations functions $A^-(r, t)$ and $I^-(t)$ correspond to the LMM while functions $A^+(r, t)$ and $I^+(t)$ correspond to the MMM. Because the correlation increase of LMM leads to negative values of $A^-(r, t)$ for some particular distances r , we have added an absolute value in the integration of $A^-(r, t)$. Functions $A(r, t)$ represent the correlation increase between molecules of approximately the same mobility, and distant of r . Functions $I(t)$ represent then the global increase of the correlation between molecules of high (I^+) or low (I^-) mobility. $I(t)$ is then related to the number of molecules aggregating and to the

size of the aggregation. For all these reasons we will name here this function $I(t)$: Intensity of the aggregation.

Figures 2a and b show the intensities of the aggregations of the least $I^-(t)$ and the most $I^+(t)$ mobile molecules versus time together with the NGP at the temperatures of 235 K (Fig. 2a), and 250 K (Fig. 2b). We find that the maximum of the aggregation of the most mobile molecules $I^+(t)$ and the maximum of the Non-Gaussian parameter appear at the same characteristic time t^* . Figures 2a and b show then that the Non-Gaussian parameter and the intensity $I^+(t)$ of the aggregation of MMM are related in some extent, because the characteristic times are the same (t^*), and the time evolutions of the two curves also correspond. This result confirms the hypothesis of a direct relation between the Non-Gaussian parameter and heterogeneity in supercooled liquids. In contrast Figure 2 shows that molecules of low mobility ($I^-(t)$) have a very different behavior. We find that the maximum of the aggregation of the least mobile molecules $I^-(t)$ does not appear at the same characteristic time t^* . We then find the apparition of a new characteristic time (t^-), associated to the aggregation of the least mobile molecules. This new characteristic time (t^-) is much larger than the characteristic time (t^*) associated to the Non-Gaussian parameter and to molecules of high mobility ($t^- > t^*$). However t^- is still within the time scale of the primary relaxation process named α relaxation for the temperatures studied here. The rapid evolution of t^- versus t^* may be seen in Figure 2c.

We then find that each component has its own characteristic time. The first characteristic time (t^*) is associated with the aggregation of the most mobile molecules, and the Non-Gaussian parameter. The time (t^*) may also be associated with string-like cooperative motions of the most mobile molecules. This point will be discussed further. The second characteristic time (t^-) is associated with the aggregation of the least mobile molecules. Within the temperature range studied (300 K to 235 K) we find a rapid increase of the two characteristic times (t^* and t^-) with temperature decrease. However the time associated to LMM (t^-) increases much more rapidly when the temperature decreases than the time associated to the MMM (t^*). In both cases we have checked that a modification of the percentage of mobiles or non-mobiles molecules does not affect the characteristic times values. This is in opposition with the height of the peaks that decrease when the percentages increase, an effect clearly due to the contribution of more and more non-aggregating molecules when the percentages increase.

In opposition with the results reported from the facilitation theory [14], at low temperatures, the NG parameter and the intensity of the aggregation $I^-(t)$ versus time have a different shape. However the maximum intensities of the aggregation of MMM $I^+(t^*)$ and of the aggregation of LMM $I^-(t^-)$ have roughly the same values. This result leads to the question of a possible relation between the two kinds of heterogeneities. However this question is still opened. We have observed these results for all the temperatures studied. The difference between the two characteristic times increases when the temperature

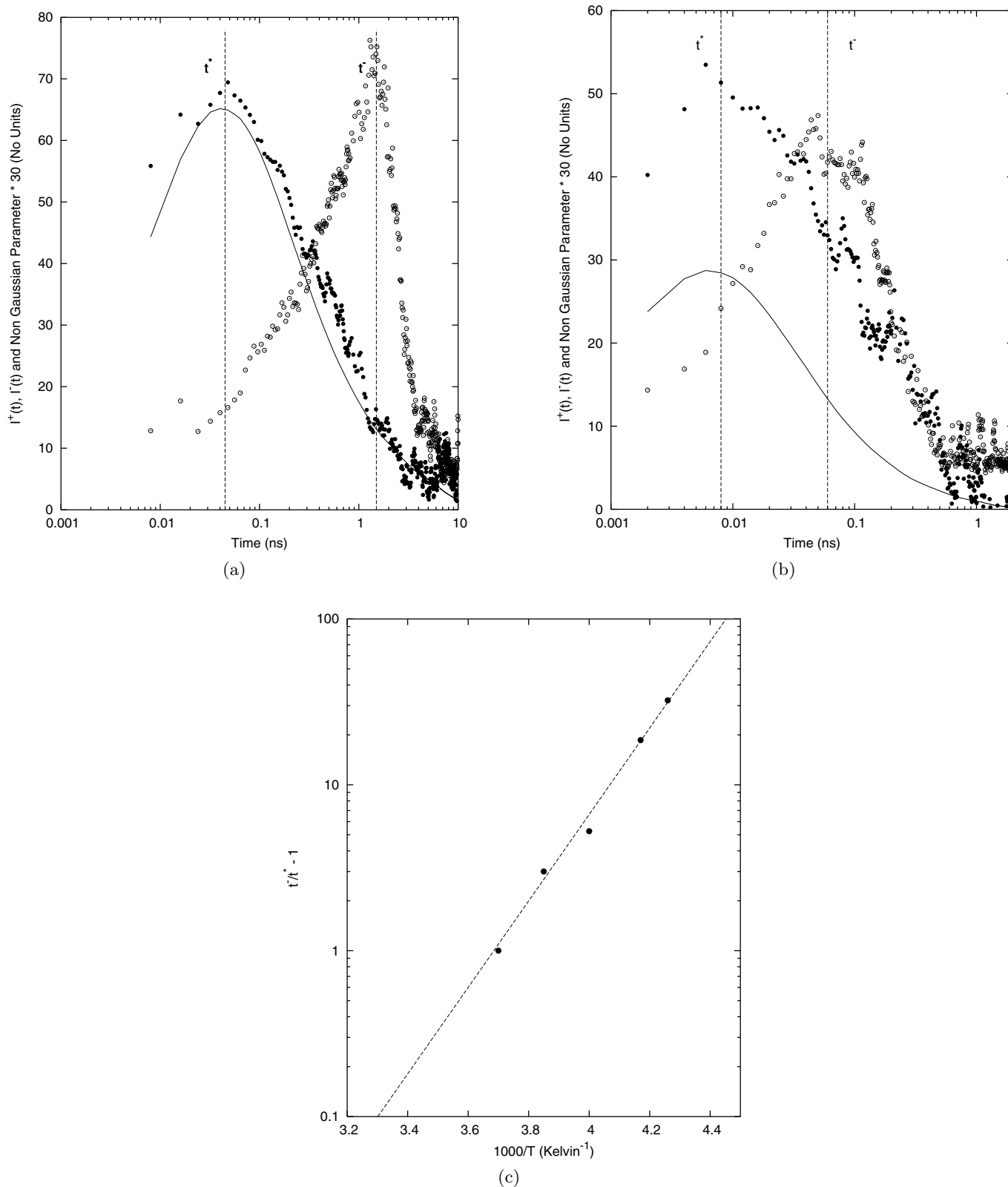


Fig. 2. (a) Functions $I^-(t)$ (empty circles) and $I^+(t)$ versus time (full circles) for the 6 percent least ($I^-(t)$) or most ($I^+(t)$) mobile molecules together with the Non-Gaussian parameter $\alpha_2(t)$ (continuous line) at a temperature of 235 K. $\alpha_2(t)$ is here multiplied by a factor 30. (b) As Figure 2a but at a temperature of 250 K. (c) Ratio of characteristic times $t^-/t^* - 1$ corresponding to the water molecule motion versus $1000/T$ where T is the temperature in kelvin.

decreases. The difference between the shapes of the two peaks increases when the temperature decreases. At low temperature the peak of $I^-(t)$ is broader in logarithmic scale than the peak of $I^+(t)$. At a temperature of 300 K the two curves ($I^+(t)$ and $I^-(t)$) do coincide. Then when the temperature decreases the intensity of the aggregation of the LMM shifts more rapidly to longer times than the other curve. The observation that the aggregation intensities $I^+(t)$ and $I^-(t)$ are equal at high temperature seems to confirm a possible relation between the two kinds of heterogeneities.

We will now investigate the presence of string-like dynamics in supercooled water with the TIP5P potential. String-like dynamics has been reported in various glass-formers, experimentally [9,19] and with MD simulations [20,24]. In these supercooled glass-formers, molecules of high mobility are following each other in a characteristic time t (usually t^*). This dynamics seems to be a characteristic of dynamical heterogeneity in supercooled liquids. String-like dynamics has been reported very recently to be present in supercooled water [25] from MD simulations with the simpler SPCE extended simple point charge potential [26]. The same behavior has also been observed from the inherent structures viewpoint [23]. However it seems important to verify the presence of this dynamics in supercooled water with the new five sites TIP5P potential [15]. In order to characterize and compare the dynamics of the different heterogeneities, we will also investigate here the dynamics of the least mobile molecules. We will then now investigate the presence of string-like dynamics for the MMM and the LMM. For this purpose we calculate the distinct Van Hove auto-correlation function $G(r, t)$. This function represents the probability to find a molecule at time t , at a distance r from the position of another molecule at time zero. We define $G_{lm}(r, t)$ for the LMM and $G_{mm}(r, t)$ for the MMM. String-like dynamics results in a sharp increase of $G(r, t)$ at $r = 0$ when t approaches the characteristic time of the strings. This characteristic time corresponds to the mean time for the replacement of one molecule by another inside a string. Figure 3a shows a sharp increase of $G_{mm}(r, t)$ at $r = 0$ with a characteristic time t^* for the MMM. It should be noted that oxygen and hydrogen mobile atoms present independently this sharp increase. In contrast in Figure 3b we do not find the same behavior for the LMM for the characteristic time (t^-). Instead the first maximum of $G_{lm}(r, t)$ only broadens when t increases. String-like dynamics is then associated only with the MMM in our simulations. This result is in agreement with the facilitation theory predictions [14]. The heterogeneities associated with the MMM and the LMM correspond then to different motions and different characteristic times.

Figure 4 shows the HO..H angular distribution functions for the least mobile (full circles), the most mobiles (empty circles) and mean molecules (continuous line) at a temperature of 235 K. In our notation in HO..H the two points correspond to the hydrogen bonding between two molecules. In dashed line we have plotted for comparison the angular distribution corresponding to a totally disor-

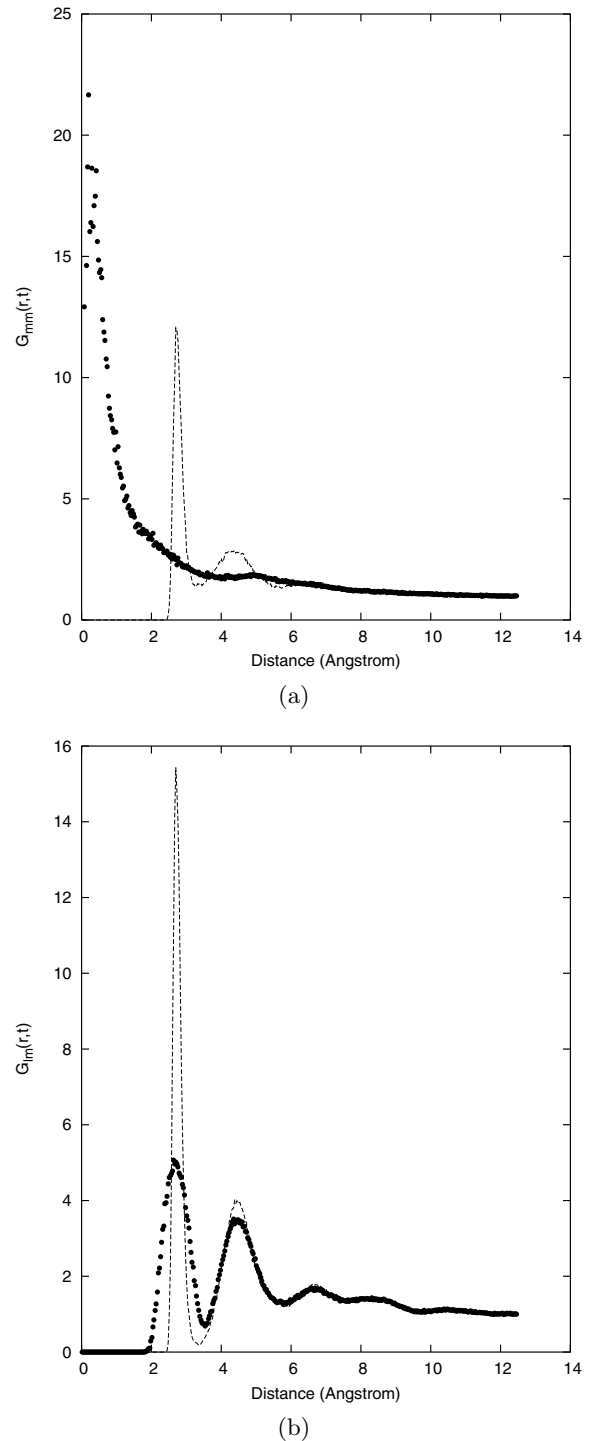


Fig. 3. (a) Distinct part of the Van Hove correlation function $G_{mm}(r, t^*)$ (full circles) and $G_{mm}(r, 0)$ (dashed line) between: the 6 percent most mobile oxygen atoms at a temperature of 240 K. $t^* = 28$ ps is the time corresponding to the maximum of the Non-Gaussian parameter for oxygen at a temperature of 240 K. (b) Distinct part of the Van Hove correlation function $G_{lm}(r, t^-)$ (full circles) and $G_{lm}(r, 0)$ (dashed line) between: the 6 percent least mobile oxygen atoms at a temperature of 240 K. $t^- = 500$ ps is the time corresponding to the maximum of the aggregation of the least mobile molecules (maximum of $I^-(t)$) at a temperature of 240 K.

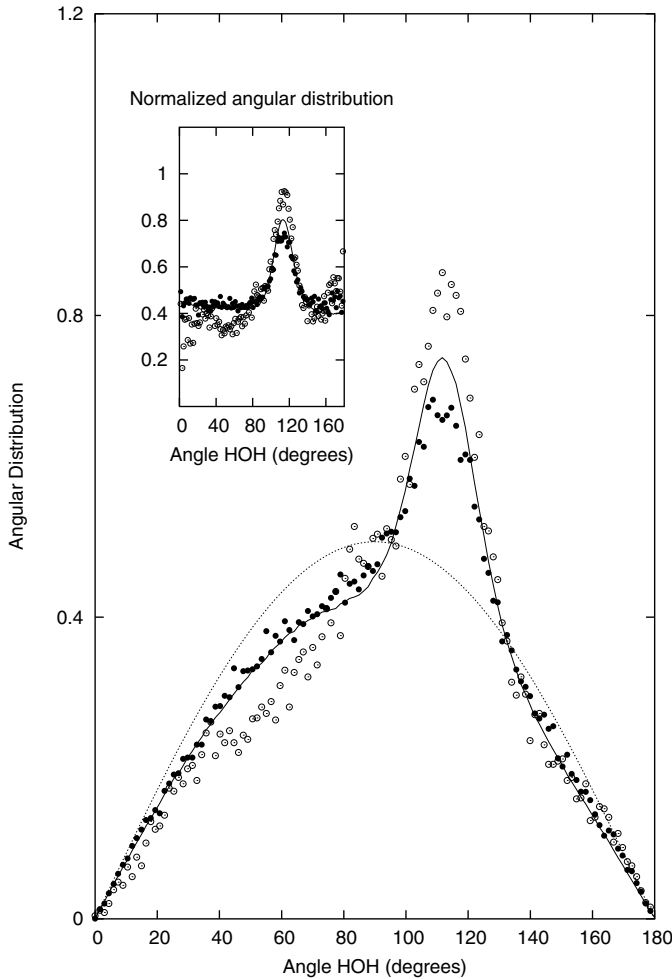


Fig. 4. Angular distribution function of the angle H-O..H between: the 5 percent most mobile (full circles), the 5 percent least mobile (empty circles) or mean (continuous line) atoms at a temperature of 235 K. The dashed line represents the solid angle distribution. The 5 percent most or least mobile molecules are selected from the mobility of each molecule i : $\mu_i(t)$ with $t = t^* = 45$ ps for the most mobile molecules and $t = t^- = 1500$ ps for the least mobile molecules. Inset: Same angular distribution divided by the solid angle distribution.

dered medium i.e. to the solid angle distribution. The inset shows the same angular distribution functions divided by the solid angle distribution. We find in Figure 4 a slight increase of angular order for the least mobile molecules and a decrease of this angular order for the most mobile molecules in comparison with the mean. The probability of finding the angles HO..H equal to their mean values is higher for the least mobile molecules (empty circles) and lower for the most mobile molecules (full circles). We then find that the least mobile molecules have more defined orientations and are then more ordered than the mean molecules while the most mobile molecules have less defined orientations and are less ordered than the mean molecules. This behavior is emphasized in the inset where the distribution functions are divided by the solid angle distribution. Empty circles representing the least mobile

molecules are here clearly higher than the continuous line representing the mean molecule while the full circles representing the most mobile molecules are lower. The observed structure is still the structure of liquid water even if the least mobile molecules have higher angular and structural correlations than the bulk. We then find an aggregation of the least mobile water molecules with more defined angles and structure but with the structure of the liquid. On the other hand we find an aggregation of the most mobile molecules with less defined angles and structure, while the mean molecules do not aggregate.

4 Conclusion

Using the new TIP5P potential we found dynamical heterogeneity in supercooled water and string-like dynamics for the most mobile molecules. The time evolution of the intensity of the aggregation of molecules of high mobility has been found to follow the time evolution of the Non-Gaussian parameter. The characteristic times associated to the Non-Gaussian parameter, string-like motions and the aggregation of the most mobile molecules have been found to coincide for supercooled water in the temperature range studied. More interestingly to us we also found a dynamical aggregation of the least mobile molecules. A new characteristic time is found, associated with the aggregation of molecules of low mobility. The two kinds of dynamical aggregation appeared then to be very different. Characteristic times are different and evolve differently. String-like motions appear only for the most mobile molecules, a result predicted by the facilitation theory [14]. In opposition with the predictions of the facilitation theory however, the timescale for the decay of the non-Gaussian parameter is found to be different from the decay of the clusters of low mobility. The aggregation of the least mobile molecules is more organized than the bulk while the opposite is observed for the most mobile molecules. However the intensity of the aggregations of the same percentage of least and most mobile molecules are roughly equals in the temperature range studied here. Moreover at the melting temperature the two curves coincide. These results open then the question of a possible correlation between these two kinds of heterogeneities. The rapid time evolution of the aggregation of molecules of low mobility when temperature decreases opens also the question of a possible correlation with fragility. Work is in progress to answer these questions.

We would like to thank Gilles Tarjus for an interesting discussion at the beginning of this work.

References

1. K. Ito, C.T. Moynihan, C.A. Angell, *Nature* **398**, 492 (1999)
2. C.A. Angell, in *Relaxations in Complex Systems*, edited by K.L. Ngai, G.B. Wright (US Office of Naval Research, Arlington, 1984), p. 3

3. C.A. Angell, *Science* **267**, 1924 (1995)
4. C.A. Angell, *J. Non-Cryst. Sol.* **131-133**, 13 (1991)
5. M.D. Ediger, *Annu. Rev. Phys. Chem.* **51**, 99 (2000)
6. D. Kivelson, G. Tarjus, *J. Non-Cryst. Sol.* **235-237**, 86 (1998)
7. V. Teboul, C. Alba-Simionesco, *J. Phys.: Condens. Matter* **14**, 5699 (2002)
8. B.M. Erwin, R.H. Colby, *J. Non-Cryst. Sol.* **307-310**, 225 (2002)
9. H. Sillescu, *J. Non-Cryst. Sol.* **243**, 81 (1999)
10. W. Kob, C. Donati, S.J. Plimpton, P.H. Poole, S.C. Glotzer, *Phys. Rev. Lett.* **79**, 2827 (1997)
11. K. Kim, R. Yamamoto, *Phys. Rev. E* **61**, R41 (2000)
12. R. Yamamoto, A. Onuki, *Phys. Rev. Lett.* **81**, 4915 (1998)
13. A. Kerrache, V. Teboul, D. Guichaoua, A. Monteil, *J. Non-Cryst. Sol.* **322**, 41 (2003)
14. J.P. Garrahan, D. Chandler, *Phys. Rev. Lett.* **89**, 35704 (2002); S. Whitelam, L. Berthier, J.P. Garrahan, *Phys. Rev. Lett.* **92**, 185705 (2004); L. Berthier, D. Chandler, J.P. Garrahan, *Europhys. Lett.* **69**, 320 (2005)
15. M.W. Mahoney, W.L. Jorgensen, *J. Chem. Phys.* **112**, 8910 (2000)
16. M.W. Mahoney, W.L. Jorgensen, *J. Chem. Phys.* **114**, 363 (2000)
17. D. Paschek, *J. Chem. Phys.* **120**, 6674 (2004)
18. M. Yamada, S. Mossa, H.E. Stanley, F. Sciortino, *Phys. Rev. Lett.* **88**, 195701 (2002)
19. A.H. Marcus, J. Schofield, S.A. Rice, *Phys. Rev. E* **60**, 5725 (1999)
20. C. Donati, J.F. Douglas, W. Kob, S.J. Plimpton, P.H. Poole, S.C. Glotzer, *Phys. Rev. Lett.* **80**, 2338 (1998)
21. M.P. Allen, D.J. Tildesley, *Computer simulation of liquids* (Oxford University Press, New York, 1990)
22. H.J.C. Berendsen, J.P.M Postma, W. Van Gunsteren, A. DiNola, J.R. Haak, *J. Chem. Phys.* **81**, 3684 (1984)
23. F. Sciortino, A. Geiger, H.E. Stanley, *Nature* **354**, 218 (1991); N. Giovambattista, F.W. Starr, F. Sciortino, S.V. Buldyrev, H.E. Stanley, *Phys. Rev. E* **65**, 041502 (2002)
24. V. Teboul, A. Monteil, L.C. Fai, A. Kerrache, S. Maabou, *Eur. Phys. J. B* **40**, 49 (2004)
25. N. Giovambattista, S.V. Buldyrev, F.W. Starr, H.E. Stanley, *Phys. Rev. Lett.* **90**, 5506 (2003)
26. H.J.C. Berendsen et al., *J. Phys. Chem.* **91**, 6269 (1987)